sustainability

MDPI

Article

Inaccuracies and Uncertainties for Harmonic Estimation in Distribution Networks

Muhammad Naveed Iqbal [1,*], Lauri Kütt [2], Kamran Daniel [2,*], Noman Shabbir [2], Anas Amjad [1], Abdul Waheed Awan [1] and Majid Ali [1]

[1] Department of Engineering, School of Digital, Technology, Innovation & Business, Staffordshire University, Stoke-on-Trent ST4 2DE, UK; a.amjad@staffs.ac.uk (A.A.); a.awan@staffs.ac.uk (A.W.A.); majid.ali@staffs.ac.uk (M.A.)

[2] Department of Power Engineering and Mechatronics, Tallinn University of Technology, Ehitajate tee 5, 19086 Tallinn, Estonia; lauri.kutt@taltech.ee (L.K.); noman.shabbir@taltech.ee (N.S.)

* Correspondence: naveed.iqbal@staffs.ac.uk (M.N.I.); kamran.daniel@taltech.ee (K.D.)

Abstract: The proliferation of electronic loads has led to a substantial increase in harmonic emissions within low-voltage distribution networks. The accurate estimation of the expected levels of harmonics in a network is a daunting task for network operators. Stochastic-based harmonic estimation models can offer a comprehensive assessment of the expected levels of harmonics in the presence of existing and future loads, including electric vehicles and smart-grid-enabled devices. Such models offer a valuable tool for network operators to assess the potential impact of harmonics on future networks and to create sustainable design solutions to meet the increasing demand for electricity while achieving net zero targets. However, several variables associated with these estimations models involve a level of uncertainty due to their stochastic nature, leading to inaccuracies in the estimations. This paper aims to provide a more realistic estimate of these uncertainties in order to improve the outcomes of harmonic estimation models for the development of sustainable distribution networks.

Keywords: harmonic estimations; load modeling; cable impedance; network uncertainties

Citation: Iqbal, M.N.; Kütt, L.; Daniel, K.; Shabbir, N.; Amjad, A.; Awan, A.W.; Ali, M. Inaccuracies and Uncertainties for Harmonic Estimation in Distribution Networks. *Sustainability* **2024**, *16*, 6523. https://doi.org/10.3390/su16156523

Academic Editor: Bowen Zhou

Received: 12 June 2024
Revised: 22 July 2024
Accepted: 28 July 2024
Published: 30 July 2024

1. Introduction

In recent years, researchers have focused on the increasing level of harmonic emissions in low-voltage distribution networks [1]. While the existing levels of harmonic emissions are still manageable for network operators, they are expected to increase significantly in the near future due to widespread usage of power-electronic-based loads, electricity generation within distribution networks, and battery charging circuits, such as those used for electric vehicles [2]. Net-zero targets for emission reduction will increase distributed electricity generation using renewables, to support a greener and sustainable future, but further increase the harmonic levels in the grid. These higher harmonic emission levels may cause several problems for utilities, in terms of overloading the distribution transformers, malfunctioning protection equipment, and increased neutral current and voltage levels in the feeders [3]. In order to address these issues, network operators are keen to understand how these increasing levels of emissions will affect both existing and future distribution networks. However, accurate estimation of harmonic levels is quite challenging, due to the various stochastic variables involved [4]. These uncertainties have received increased attention recently because of the rapid integration of renewable electricity generation into the power system [5]. The objective of this paper was to assess and measure the influence of these variables on current harmonic estimates. The accurate assessment of harmonic emission will help network operators in the operation, planning, and expansion of distribution networks, to accommodate net zero emission targets for a more sustainable electrical power network [6].

Traditionally, researchers have studied the impact of current harmonics on distribution networks by analyzing measurement data [7]. Various approaches have been used for this purpose, including recording of power quality measurement data at various points within the distribution network [8]. These measurements can be taken at the distribution transformer to gauge the overall impact. Another method is to measure at the point of common coupling (PCC) for individual buildings and then compare these results with measurements taken at the distribution transformer to determine the effects of harmonic cancellation [9]. However, gathering and processing such large-scale measurements is challenging, due to the enormous size of distribution networks [10]. Furthermore, predicting future harmonic emissions based on measurement data alone is likely to be inaccurate. Another way to approach the problem of harmonic emission assessment is developing probabilistic harmonic estimation models [11]. Several models are available in the literature, which can be broadly classified as numerical and probabilistic methods [12]. The numerical models can be categorized as frequency- and time-domain models [13]. These models provide a deterministic assessment of individual circuits but have limitations such as their inability to handle the interdependency of current harmonics on the voltage waveform and harmonics [14]. The probabilistic approach, on the other hand, is more suitable because of the short-term, random, and intermittent nature of residential loads [7]. Typically, two probabilistic approaches are commonly found in the literature, bottom-up load-based models and load-measurement-based models. The bottom-up model uses an analytical approach to simulate the harmonic injection by simulating load states and estimating the aggregated emissions [15,16]. The measurement-based approach uses probability distributions to represent aggregated harmonic emission data at the PCC [17].

The harmonic estimation modeling techniques described above typically neglect the majority of uncertainties and inaccuracies associated with the real-time behavior of the connected load and the distribution network. Figure 1 shows different types of measurement and modeling uncertainties that can impact the outcome of harmonic estimation models.

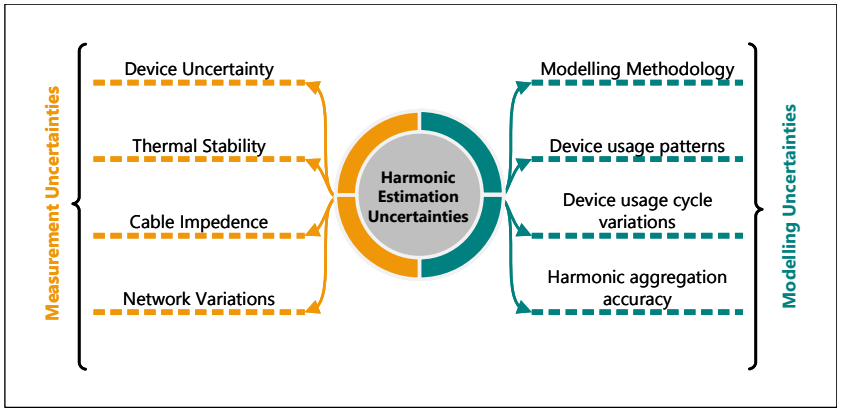

Figure 1. Classification of uncertainties and inaccuracies in harmonic estimation.

The variability in the load connected to the network is due to the stochastic behavior of end-user load usage [18]. Furthermore, there are various types of loads that can be classified based on their circuit topologies or the nature of the current they draw from the network. The type and amount of load are different in each household, and the usage behavior of the occupants results in a dynamic profile of harmonic emissions from each household. The harmonic emission is subjected to harmonic cancellation within the electrical circuit of the household and also at the PCC [19]. As several households are connected to the low-voltage end of the distribution network, their collective emissions may result in further aggregation of individual harmonic components as well as be subject to variation in the supply voltage on the distribution network side [20]. Measurement uncertainties include device uncertainty and accuracy margins, as well as various variations in the measurement data. These variations typically correspond to the thermal instability of the loads during

power quality measurements and the impact of cable impedances on the harmonics. The dynamic conditions of the network in terms of voltage harmonics also cause variations in current harmonic emissions from the loads. These variations and uncertainties at various levels in the modeling and measurements influence the estimation of harmonic emissions. Therefore, it is crucial to assess these variations, uncertainties, and inaccuracies, to construct a reliable model that can provide more accurate harmonic level estimates.

In this paper, we have presented most of the uncertainties and inaccuracies that may impact the output of harmonic estimation models and also quantified their values. In Section 2, a brief overview of the stochastic harmonic emission model (SHEM) is discussed. Section 3 discusses various uncertainties and the methodology to quantify their values. The conclusions are discussed in Section 4.

2. SHEM Model and Measurement Setup

In the previous section, we discussed various harmonic estimation modeling approaches found in the literature. While these approaches effectively address sporadic variations, they have limitations in terms of accuracy and computational complexity. To overcome these limitations, combining current harmonic measurements with a device-level aggregation approach could yield better results. This combined approach would be able to handle the randomness of device usage patterns, measurement inaccuracies, and harmonic emission variations. It is essential to incorporate every possible inaccuracy and uncertainty in the model, to ensure a more accurate estimation.

Our proposed SHEM model is based on three main sections. A high-resolution measurement database, a stochastic device usage model, and bivariate harmonic analysis. The details of this proposed method were previously described in [12]. As the scope of this paper is limited to discussing the various uncertainties and inaccuracies that may have a significant impact on SHEM models, we only use a small part of our model that provides harmonic estimation of the lighting load for 60 households. An abstract diagram of our SHEM model is shown in Figure 2.

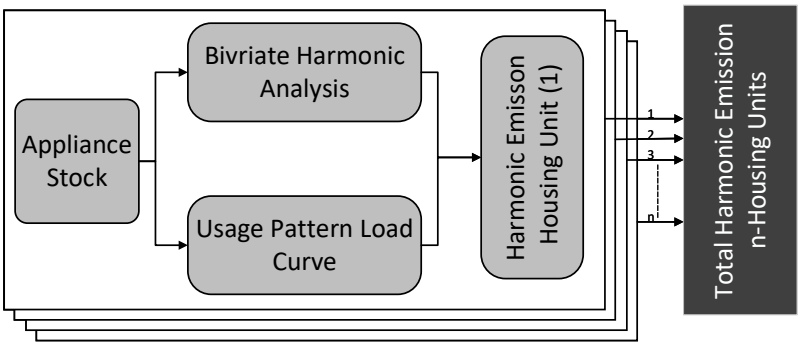

Figure 2. Block diagram of proposed SHEM model [12].

We used a broad measurement database that includes power quality measurements of several end-user loads at various voltage waveforms. To automate the process of measurement, we used a test bench capable of recording power quality indices of 16 loads at a time on several voltage waveforms. The test bench included a power quality measurement device, PQ Box 200 (A-Eberle, Nürnberg, Germany), having a sampling frequency of 41 kHz. It further included a National Instrument (NI) data acquisition (DAQ) board that provided digital input to a control box based on the signal generated using a MATLAB program. The control box includes relays to control the loads. We used two different programmable power sources, a 1.7 kVA Omicron C356 and 4 kVA Chroma 61505. A reference signal to control the output of these programmable power supplies was also generated from the DAQ board using the MATLAB program. Figure 3 provides a block diagram representation of our measurement setup.

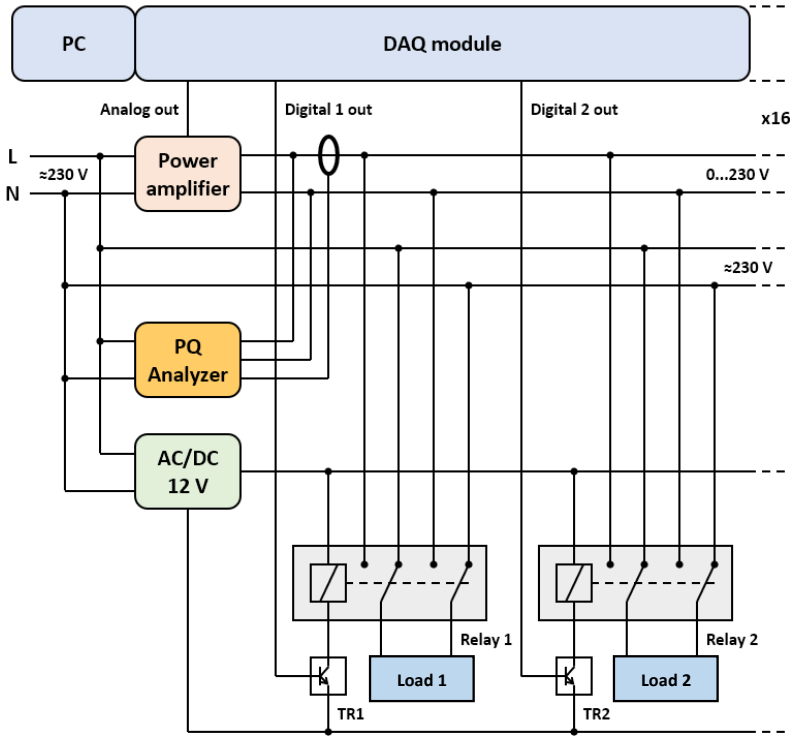

Figure 3. Block diagram of PQ measurement setup.

3. Elements of Uncertainties and Inaccuracies

The estimation results of current harmonic emissions obtained from SHEM models can be affected by uncertainties and inaccuracies due to various random variables and assumptions used in the models. These uncertainties can be categorized into measurement uncertainties and load modeling uncertainties. A detailed discussion and possible quantification of these uncertainties is explained in the following sections.

3.1. Measurement Uncertainties

The measurement uncertainties include possible inaccuracies that may penetrate into the measurement results from the measurement setup. These may include calibration errors, power quality analyzer uncertainty margins, and uncertainties added by auxiliary measurement devices. Furthermore, the thermal stability of the load also adds significant variations to the harmonic measurement results of the devices [21]. The cable attached to the end user devices also alters the magnitude and phase angles of current harmonics to a certain extent [22].

3.1.1. Measurement Setup Inaccuracies and Uncertainties

SHEM models are based on stochastic analysis of measurement databases, including power quality measurements of end-user loads recorded at different voltage waveforms. A measurement setup involves a programmable power supply and a device for measuring power quality indices, which form the central part of the setup, as described in Section 2. The accuracy of the measurement setup is of utmost importance, as it affects the harmonic estimations derived from the results of the measurement instruments commonly found in academic and research labs. The reliability of these instruments is often based on their calibration, which is a costly procedure that is mostly performed by third-party organizations having accredited lab facilities. However, the calibration certificate provided after the process usually does not cover the full spectrum of readings provided by the instrument. For instance, the phase angle calibration of power quality measurement devices is not included in most calibration procedures. Additionally, this process will only cover

the measurement instrument and not auxiliary equipment, such as test boards and control units, etc. used in the measurement.

We have created a technique using metrology principles and signal processing to determine the precision of our measurement setup. This technique can assess the uncertainty and inaccuracy of the entire measurement setup, including the power quality measurement device, PQ Box 200, and other auxiliary equipment that contribute to voltage waveform generation. It involves a two-step approach, where the accuracy of the power quality measurement instrument is calculated by comparing it with a reference instrument in an accredited calibration facility. Figure 4 shows the process of accuracy evaluation for the measurement setup. The calibration setup includes a current waveform generator, current transformer, and wattmeter consisting of two multi-meters. Table 1 shows the details of the calibrated equipment used in this experiment.

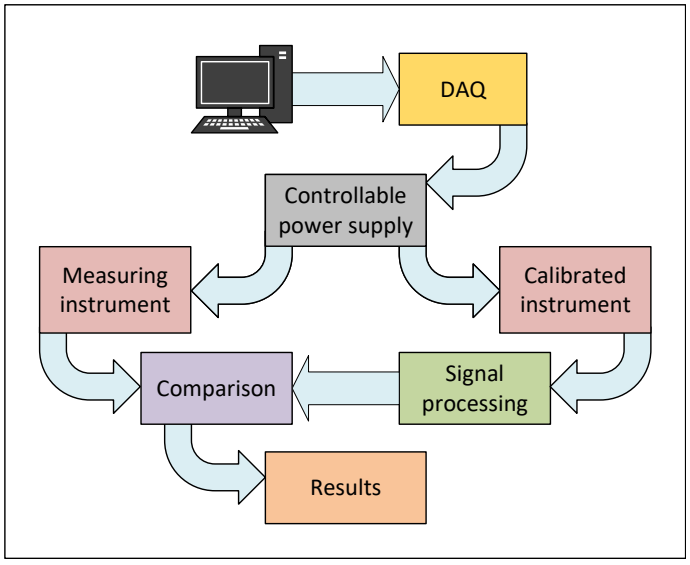

Figure 4. Measurement accuracy evaluation methodology.

Table 1. List of calibrated equipment in the accredited lab.

No.	Equipment	Model
1	Calibrator	CP11B
2	Current Transformer	I509
3	Watt Meter	SWM3458
4	Multimeter	Agilent 3458A
5	Software	PowerLF v1.2

We selected a list of current harmonics from our measurement portfolio, as indicated in Table 2, and generated them using the calibrated system and calibrated power quality measurement instrument. We compared the results by replacing the calibrated power quality measurement instrument with our primary power quality measurement instrument. The difference between the magnitude and phase measurements of individual harmonics is listed in Tables 3 and 4.

In the next stage, we evaluated the accuracy of our measurement setup as defined in Section 2 in the laboratory. We compared the measurement results of the PQ Box 200 with a reference instrument, "Keysight 34465A," which is capable of recording voltage and current waveforms at a sampling rate of 50 kHz. The current measurements were obtained using a 12 ohm shunt resistor, with the same set of voltage harmonics as the input data used in the previous experiment. The recorded current waveforms from the reference instrument were analyzed using discrete Fourier transform (DFT) to extract phase and magnitude values of the current harmonics. The difference in RMS values of the individual

harmonics generated through the measurement setup and measured by the primary and reference instrument (Keysight 34465A) was calculated. The correction factor indicated in Table 5 shows the inaccuracies and uncertainties added by the auxiliary components in the measurement setup. The correction difference represents the uncertainty added by the auxiliary equipment, as the uncertainty of the primary measurement instrument (PQ Box 200) had already be taken into account.

Table 2. Harmonic RMS (A) and phase angle (degree) values of selected signals.

Harmonics	Signals									
	1		2		3		4		5	
	Irms	Phase	Irms	Phase	Irms	Phase	Irms	Phase	Irms	Phase
1	0.106	-	0.045	-	0.081	-	0.036	-	0.037	-
3	0.085	—	0.037	-	0.066	−98.5	0.015	11.7	0.035	−136.3
5	0.069	-	0.028	-	0.044	142.0	0.006	55.1	0.031	73.4
7	0.050	-	0.020	-	0.024	39.9	0.004	53.7	0.025	−75.7
9	0.034	-	0.013	-	0.017	−38.1	0.003	87.7	0.019	137.4
11	0.024	-	0.010	-	0.016	−130.2	0.002	99.0	0.014	−5.4
13	0.022	-	0.008	-	0.013	130.7	0.002	120.7	0.009	−140.1
15	0.022	-	0.007	-	0.010	43.2	0.002	142.6	0.006	96.7
17	0.020	-	0.006	-	0.010	−43.3	0.002	156.3	0.006	−23.8
19	0.018	-	0.006	-	0.009	−138.6	0.001	−178.1	0.006	−153.2

Table 3. Percentage difference between harmonic magnitude measurements between primary and reference instrument.

Harmonic	Signal 1	Signal 2	Signal 3	Signal 4	Signal 5
No.	Current (A%)				
3	−0.36	−0.24	−0.32	−0.33	−0.32
5	−0.37	−0.29	−0.36	−0.36	−0.35
7	−0.38	−0.39	−0.37	−0.38	−0.37
9	−0.41	−0.40	−0.40	−0.41	−0.40
11	−0.47	−0.33	−0.46	−0.47	−0.45
13	−0.55	−0.38	−0.53	−0.55	−0.53
15	−0.64	−0.51	−0.63	−0.65	−0.63
17	−0.74	−0.55	−0.74	−0.74	−0.73
19	−0.83	−0.58	−0.82	−0.84	−0.82

Table 4. Absolute phase difference between primary and reference instrument measurements.

Harmonic	Signal 3	Signal 4	Signal 5
No.	Degree		
3	0.31	0.18	0.42
5	0.36	0.18	0.53
7	0.45	0.21	0.72
9	0.52	0.23	0.85
11	0.71	0.32	1.20
13	0.83	0.31	1.02
15	0.91	0.42	1.12
17	1.06	0.45	1.31
19	1.16	0.51	1.40

Table 5. Correction factor estimated for the primary instrument.

Harmonic		Measurements Differences		Correction Factor
No.	**RMS**	**Primary Instrument A(%)**	**Reference Instrument A(%)**	**A(%)**
1	0.0445	−0.5429	−0.0102	−0.6040
3	0.0363	0.1353	0.0560	0.5005
5	0.0283	0.2406	0.1563	0.6213
7	0.0196	0.3523	0.2556	0.7475
9	0.0130	0.4293	0.4255	0.8555
11	0.0091	0.7332	0.6360	1.2093
13	0.0082	0.8974	0.8990	1.4542
15	0.0071	1.1665	1.2015	1.8199
17	0.0064	1.5429	1.5559	2.2944
19	0.0055	1.9114	1.9543	2.7493

3.1.2. Thermal Stability Impact on Harmonic Measurements

The thermal stability of loads is often disregarded when measuring the current harmonic emission of loads. Research indicates that the harmonic emission profile of various loads varies significantly, depending on their thermal stability [21]. The results of harmonic estimation using measurement data of thermally unstable loads lead to significant errors. To quantify the impact of thermal instability on current harmonic measurements, we conducted an experiment.

For this purpose, switch-mode power supplies (SWMP) and LED lamps were chosen. We continuously recorded their current harmonic emission at a sinusoidal voltage of 230 V, with a resolution of 1 s over 1 h. We recorded both magnitude and phase angles, and analyzed the results to assess the impact of thermal stability. Both LED lamps and switched-mode power supplies contain power-electronic-based converters in their internal circuits. Each converter topology draws a distinct current waveform and can be classified based on this. We classified the LED lamps into four types, and their current waveforms are shown in Figure 5a. Similarly, the SMPSs were classified into two types, and their current waveforms are shown in Figure 5b.

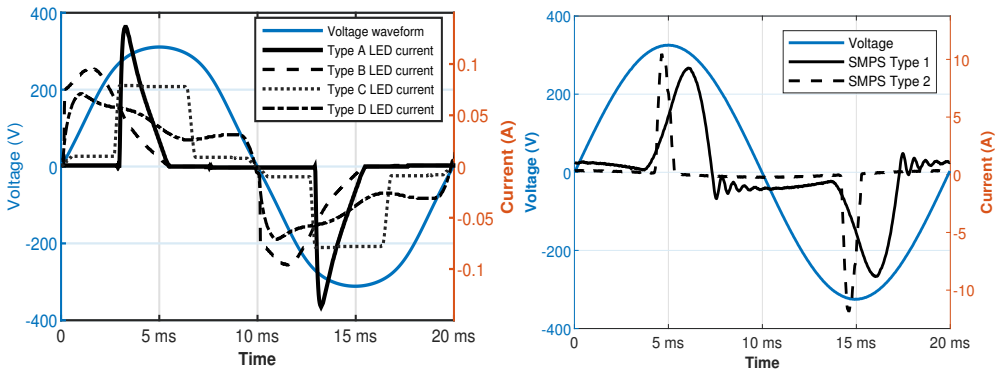

(a) **(b)**

Figure 5. Current waveform from different loads (**a**) LED lamps (**b**) Switch Mode Power Supplies.

The variation in both magnitude and phase angle overtime during the measurement of each LED lamp and SMPS was analyzed to determine the impact of thermal stability. In order to neutralize the impact of the unwanted variation that can be caused due to measurement uncertainty, we utilized a curve fitting approach. This approach not only eliminated the impact of tiny variations but also provided a mathematical framework to evaluate the thermal stability time of the devices. The exponential trend curve applied to the current harmonic variation over time is represented by Equation (1).

$$y = (Ah_f - Ah_o) \times e^{(-\frac{x}{\tau})} + Ah_f \quad (1)$$

In this equation, the variable y represents the output data for each input value of magnitude or phase angle of a specific current harmonic. Ah_f denotes the final magnitude or phase value of a particular harmonic after it reaches thermal stability. Ah_o represents the initial values of the magnitude or phase of the current harmonic. τ represents the time taken by the current harmonic magnitude and phase variation to delay or rise by the factor of e and is estimated using Equation (2).

$$\tau = \frac{T_{80} - T_o}{1 - \ln(\frac{1-\gamma}{(Ah_f - Ah_o)})} \quad (2)$$

Here, T_{80} represents the time at which either magnitude or phase change approaches 80% of its final value. γ indicates the difference between the magnitude or phase value at T_{80} and during the 1st min. After analyzing the current harmonic variation of LEDs and SMPS, it was noted that these loads achieved thermal stability after 3τ. Hence, the time required by the loads to become thermally stable was calculated using Equation (3).

$$T_s = 3 \times \tau \quad (3)$$

Figure 6 shows the variation in the current harmonic magnitude of a load over 1 h. The green line shows the RMS value of the magnitude, while the blue line represents the applied curve fitting. The red and black dots show the τ and 3τ values over the trend curve. The total harmonic distortion of the current for both LEDs and SMPS varied significantly until they reached thermal stability. Figure 7a shows the variation in the THDi of the LED lamps. While most lamps showed a THDi variation between 3 and 6%, the maximum difference was around 18%. Similarly, the SMPS data for THDi variation showed that most power supplies exhibited a difference of more than 14%, while the maximum difference was 21% between a cold and thermally stable power supply, as shown in Figure 7b.

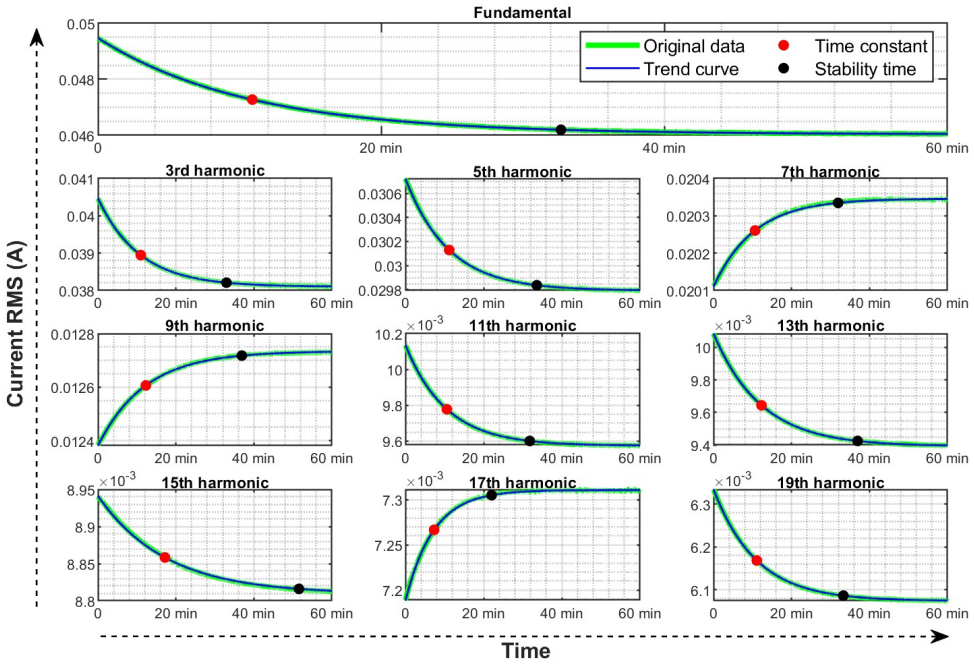

Figure 6. Current harmonic magnitude variation over time.

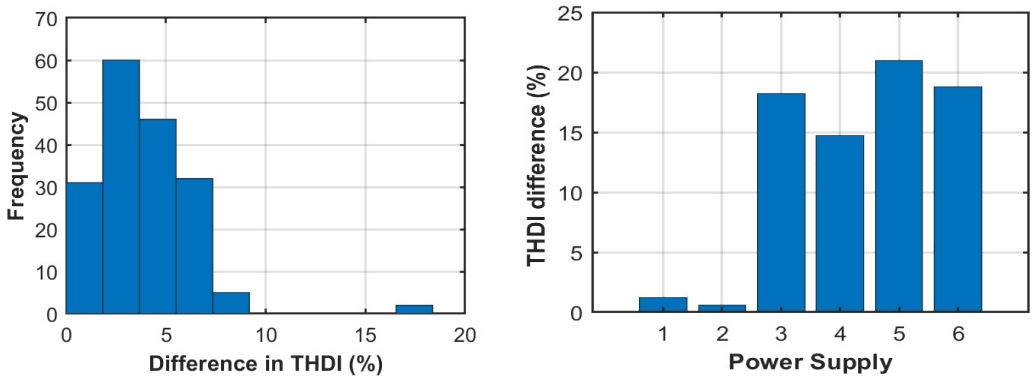

(a) **(b)**

Figure 7. Percentage THDi variation for (**a**) LED lamps, (**b**) switch mode power supplies.

To determine the time required for thermal stability, we analyzed the value of 3τ for the magnitude and phase variation of each LED lamp and SMPS. Figure 8a presents a box plot that shows the magnitude stability achieved by the different loads over time, while indicating a relationship between the mean, 5th, and 95th percentile values of stability time and harmonics. In this plot, the upper and lower whiskers are extended to the 99th and 1st percentile value of the stability time. It is evident from this figure that the majority of the load became thermally stable within 40 min. However, some loads took nearly 55 min to achieve thermal stability. The phase stability trends over time are shown in Figure 8b. While the overall stability of the phase angle variation for the 95th percentile of the load was improved in contrast to the magnitude, some loads still required up to 60 min to attain stable phase angles for certain harmonics when compared to the magnitude.

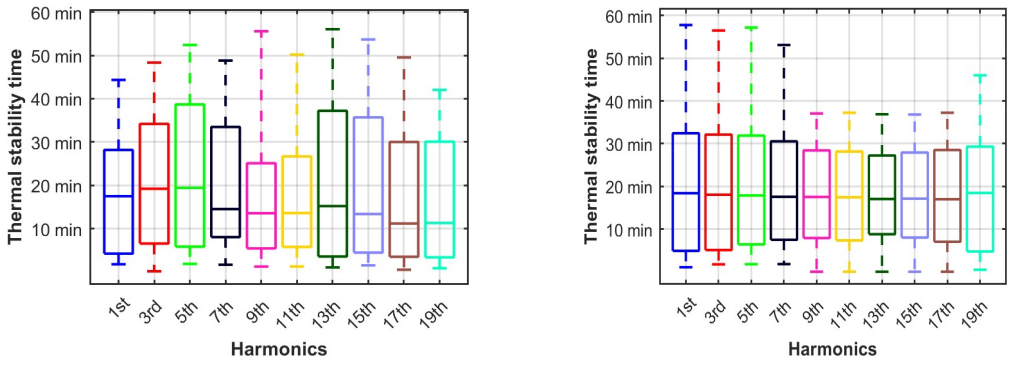

(a) **(b)**

Figure 8. Boxplot representing (**a**) magnitude thermal stability, (**b**) phase thermal stability.

3.1.3. Impact of Cable Impedance

The impact of cable impedance on current harmonics is overlooked in the existing models available in literature, despite its significant impact on both magnitude and phase angles. Although stochastic harmonic estimation models provide an opportunity to include this kind of uncertainty, the extent to which cables might affect the current harmonics is not easy to estimate. The length of the cables may vary depending on the area of the buildings, and probabilistic estimation makes more sense to quantify their impact on harmonics emissions [23].

We performed several measurements of current harmonic emission from loads, while including various lengths of cables during the experiment. LED lamps were selected as loads because of their stable harmonic emission profile. These lamps were warmed up for at least 1 h to remove any variation in their current harmonic emission profile due to thermal stability. We used three cable lengths of 10, 30, and 110 m and measured the LED

lamp's harmonic emission profile with and without attaching cables between the lamps and measurement device. For this purpose, we used a three-core stranded 1.5 mm 3G cable, which is the most commonly used cable in building electrical installation. Figure 9 shows the THDi difference for the different loads with and without cables.

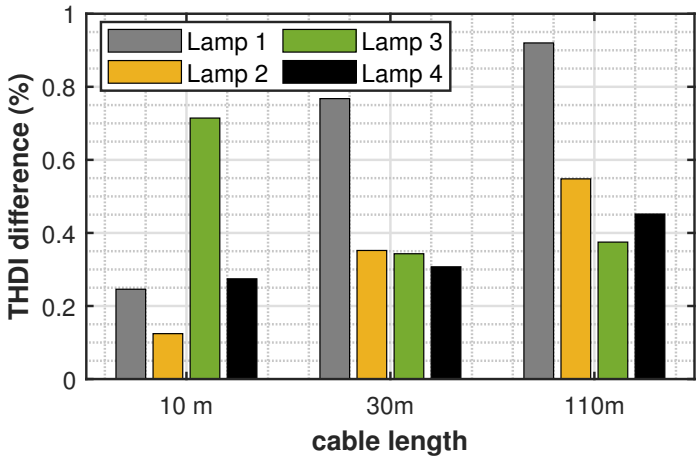

Figure 9. Percentage THDi difference of LED lamps for various cable lengths.

It is evident from the figure that the THDi difference increased with the length of the cable, where the maximum difference reached up to 0.9%. Although this difference may seem small, in real-world scenarios, cable lengths could be much longer, and the resulting impact could be more significant. Figure 10a displays a box plot that illustrates the relationship between the absolute magnitudes or phase angle variations of the different harmonics measured with and without cables. The box represents the mean, 95th, and 5th percentile values, while the whiskers extend to the extreme values. Although the difference in magnitude variation of current harmonics was not more than 0.8% with or without cables, the maximum difference could reach up to 3% for certain harmonics.

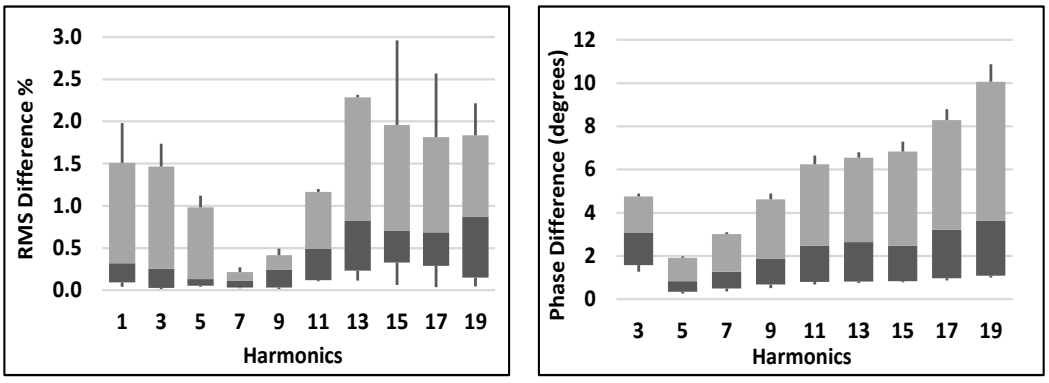

(a) **(b)**

Figure 10. Boxplot showing harmonic difference in (**a**) percentage magnitude with cables, (**b**) absolute phase difference with cables.

The phase angle measurement shows a more consistent increase in the difference as we move from lower to higher-order harmonics. The mean difference in phase angle measurements with and without cables is in the range of 0.5 to 3 degrees. However, the maximum difference is more than 10 degrees for higher-order harmonics, as shown in Figure 10b.

In order to estimate the impact of very long cables on the current harmonic variation, we used an electrical equivalent model of a 1000 m long cable. This model was based on the parameter estimated from the 3 m length of a 3G stranded 1.5 mm cable. From the resistance, inductance, and capacitance measurements of the cable, similar parameters

were estimated for a 1000 m cable. For the experiment, we used a 135 µH inductance and 13.3 ohm resistance, while the capacitance was ignored because of its small value. LED lamps were connected with these resistances, and the inductance and current harmonic emission profiles were recorded. Figure 11 shows the current waveforms for an LED lamp recorded with a 1000 m electrical model of the cable and without it. A significant difference can be seen, which shows that cable impedance can significantly alter the shape of the current waveforms drawn by loads. Table 6 summarizes the difference in both magnitude and phase when loads were measured with and without an electrical model of a 1000 m cable.

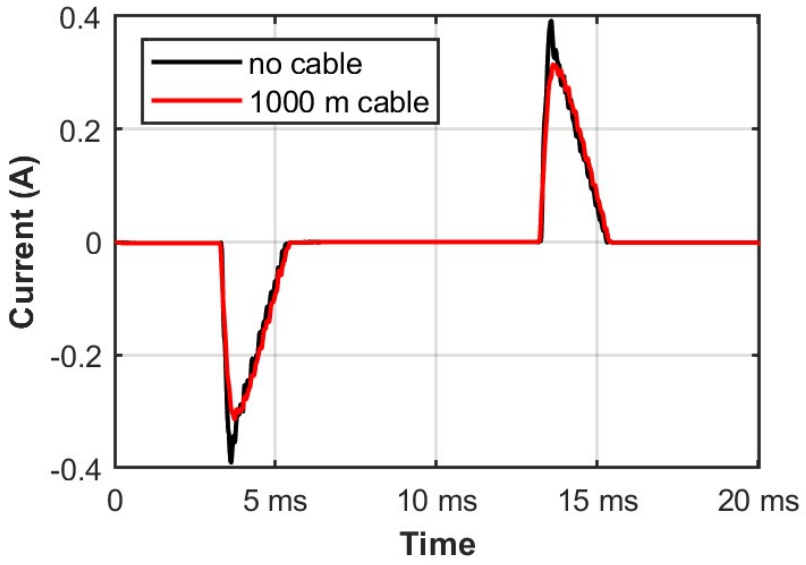

Figure 11. Variation in the current waveform of a LED lamp when measured with a 1000 m electrical model of a cable.

Table 6. Current harmonics magnitude and phase difference for a 1000 m cable [24].

	Magnitude difference for a 1000 m cable										
	THDi	$\mathbf{I}_f$	$\mathbf{I}_3$	$\mathbf{I}_5$	$\mathbf{I}_7$	$\mathbf{I}_9$	$\mathbf{I}_{11}$	$\mathbf{I}_{13}$	$\mathbf{I}_{15}$	$\mathbf{I}_{17}$	$\mathbf{I}_{19}$
Lamp 1	3.3%	0.5%	0.4%	1.3%	2.9%	5.6%	9.4%	10.6%	10.1%	12.1%	15.8%
Lamp 2	5.9%	−0.2%	0.5%	2.1%	4.9%	9.8%	17.3%	21.8%	21.3%	23.9%	30.4%
	Phase difference for a 1000 m cable										
	THDi	$\boldsymbol{\phi_1}$	$\boldsymbol{\phi_3}$	$\boldsymbol{\phi_5}$	$\boldsymbol{\phi_7}$	$\boldsymbol{\phi_9}$	$\boldsymbol{\phi_{11}}$	$\boldsymbol{\phi_{13}}$	$\boldsymbol{\phi_{15}}$	$\boldsymbol{\phi_{17}}$	$\boldsymbol{\phi_{19}}$
Lamp 1	3%	0°	3°	6°	8°	2°	11°	11.3°	13°	15°	18°
Lamp 2	5.9%	0°	5°	9°	13°	16°	18°	16°	10°	20°	23°

A THDi difference of 3 to 6% was observed for the loads when measured with or without the cable model. Furthermore, individual harmonics also showed a significant difference in both the magnitude and phase measurements with and without the cable model. This difference also increased from lower to higher order harmonics, where a maximum difference of 30.4% and 23 degrees was observed for the 19th harmonic.

3.1.4. Impact of Network Variability

The load connected to the network at the point of common coupling (PCC) changes continuously due to the stochastic nature of load usage. A network has its own set of parameters, which are also dynamic in nature. For instance, the voltage that the network

provides at the PCC can have several variations and network-induced harmonics. These harmonics are added by the network, as well as the various loads connected to it. The voltage magnitude may also fluctuate in weaker parts or at the end of long stretched radial networks. All these variations in the voltage waveform also affect the devices used by end-users [25]. The current harmonic emission profile of these devices changes as a result, which further affects the network voltage harmonic. Therefore, these variations are dynamic in nature and can have a significant impact on the outcomes of SHEM models.

To account for the unpredictability of networks in harmonic estimations, we suggest taking into consideration multiple voltage waveforms while measuring the current harmonic emissions of loads. Various studies have also implemented this approach to analyze the effect of networks on the current harmonic emissions of various loads, including electric vehicles (EVs). In our measurement process for recording current harmonic emission profiles of individual loads for the SHEM model, we used different voltage waveforms, as shown in Figure 12. Along with standard distorted waveforms such as sinusoid, flat-top and pointed-top, we included actual voltage waveforms measured in the network at different times of the day, namely VG1, VG2, and VG3, recorded in the morning, evening, and non-peak hours. We generated these waveforms using our measurement setup and measured the current harmonic emission profile of the loads. This resulted in a portfolio of measurements that enabled us to include the impact of network uncertainties in our SHEM model.

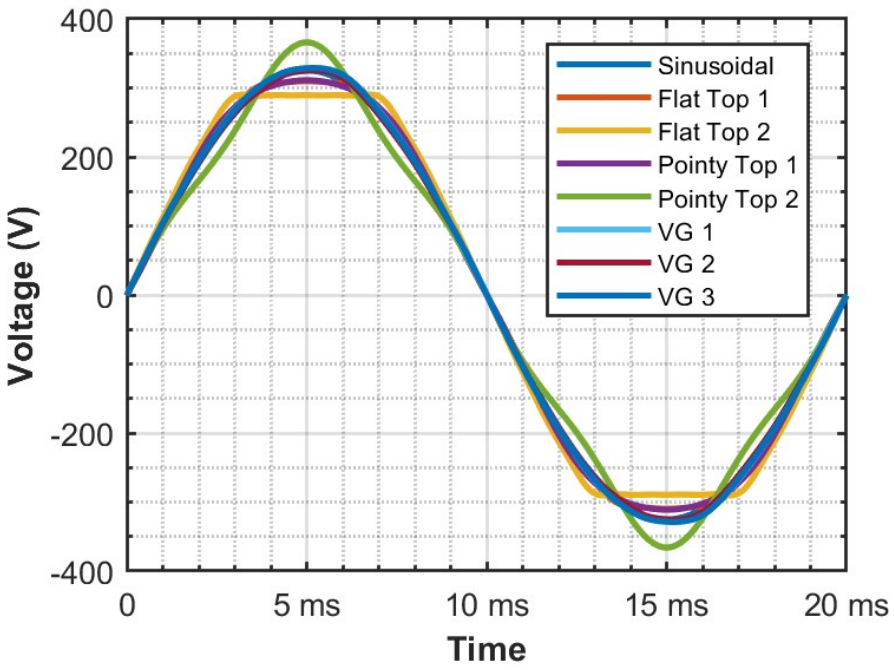

Figure 12. Different voltage waveforms used to measure harmonic emission of loads to assess the impact of network uncertainties.

To further evaluate the impact of network uncertainties, we further tested these different measurements of harmonic emission profile for the lighting usage model. Figure 13 shows the impact of network uncertainties on the 3rd harmonic current estimated using our lighting usage SHEM model. The aggregated current harmonic emission shows significant variation for the different voltage distortions. However, these impacts could be included in the SHEM model itself by using a probabilistic approach to estimate the particular result of harmonic emission at any given time. Furthermore, we also provide a band of uncertainty that can show the tolerance level expected in the outcome of the SHEM model.

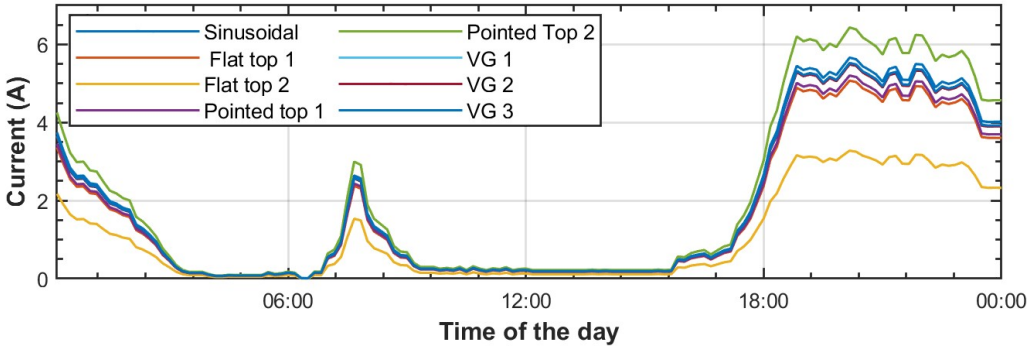

Figure 13. Impact of network variability on the magnitude of the 3rd harmonic current estimated by SHEM model.

3.2. Load Modeling Uncertainties

3.2.1. Stochastic Modeling Uncertainty

The literature has widely discussed the impact of stochastic or probabilistic methodologies on various research problems related to electric power systems [24,26]. The selection of the probability distribution for the data depends on its goodness of fit. Due to its simple computation and relatively wide application across many datasets, the normal distribution is extensively used, while other popular data distributions include Weibull, log-normal, and exponential distributions.

The modeling of load usage and harmonics poses a challenge due to the involvement of interdependent random variables. The interdependence between the magnitude and phase angle of harmonics is one such example. Similarly, for load usage modeling, several interdependent variables are involved, making the problem very challenging to tackle with the majority of the mathematically defined probability distributions. Empirical distributions provide an excellent option because of their ease of usage for almost any problem related to the modeling of random variables. The only problem is their extensive computational time, which can be easily managed with modern computational power and advanced simulation software such as MATLAB.

Equation (4) defines the empirical distribution function p_M for M independent random variables $(R_1, R_2, ...R_N)$. The p_M is a step function, and its step size is $1/M$ and value of less or equal to R.

$$p_M(R) = \frac{Sample\ data\ points \leq R}{M} \tag{4}$$

$$p_M(R) = \frac{1}{M} \sum_{n=1}^{M} \mathbf{I}(R_n \leq R) \tag{5}$$

$\mathbf{I}(X_n \leq X)$ is the indicator function and will be equal to 1 if $(R_n \leq R)$ and zero in other cases.

The selection of the data distribution function is the most crucial aspect of any stochastic modeling problem. The correct choice will generate more accurate results in comparison to the input dataset. We made a comparison of several distributions that showed a close fit to the appliance usage dataset and the empirical distribution. Figure 14 shows a comparison of normal distribution and empirical distribution applied to a dataset related to lighting usage. The selected data represented the duration of lighting usage in households where the amount of lighting usage was constant during each interval. The normal distribution provided the closest fit based on the MATLAB distribution fit functions.

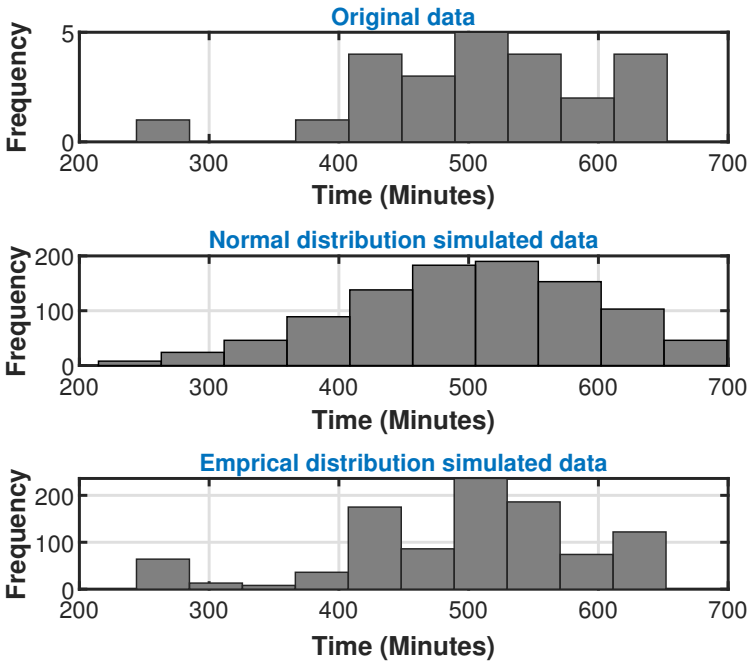

Figure 14. Impact of network uncertainties on the magnitude of the 3rd harmonic current estimated by the SHEM model.

The results shown in Figure 14 indicate the efficiency of the empirical distribution function in the context of generating data points that showed similar histograms to the original dataset. Hence, the empirical distribution is more practical for SHEM models, as they are based on large datasets with high visibility and clustered data.

3.2.2. Device Usage Pattern Variations

Modern appliances integrate power-electronics-based power supplies that offer efficient power management and control. These power supplies enable better control of motors, which are essential components of many end-user devices. Advanced motor control circuits and inverter-based circuits can provide a wide range of torque–speed characteristics, allowing end-user devices to perform tasks more efficiently. These devices typically break a task into several sub-tasks and inject a distinct harmonic fingerprint for each sub-task. Vacuum cleaners, dishwashers, and washing machines are a few examples of similar end-user appliances. These devices come with multiple pre-programmed operating modes, each consisting of several sub-cycles that provide the user with better control over the device. However, predicting the harmonic emission of these devices is challenging, as each user may use the device according to their preference, resulting in significant variations in their contribution of harmonic injection into the grid. Figure 15 shows the 3rd and 5th current harmonic emissions of a dishwasher measured on a sinusoidal voltage waveform. It shows a significant variation in the harmonic emission over the whole cycle of operation for the dishwasher.

Electronic appliances such as TVs, laptops, and computers also perform a lot of tasks where the power consumption requirements change significantly. As a result, the harmonic emission profile is also not constant for these types of devices.

A typical SHEM model includes several appliances in each household, and therefore it is important to consider the harmonic emission profiles of appliances measured over the entire cycle rather than for a few minutes during their operation. This practice is more related to real-world scenarios and can provide better results for harmonic emissions.

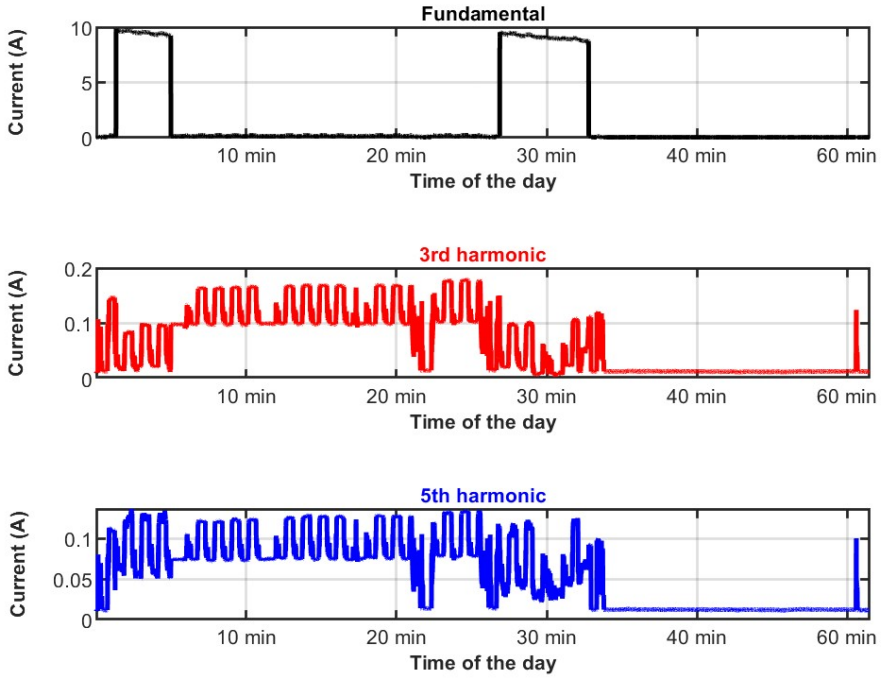

Figure 15. Harmonic emission variation of a dishwasher over different modes of its operation.

3.2.3. Harmonic Aggregation Uncertainties

It is important to consider harmonic cancellation while modeling harmonic emissions. The point of common coupling connects several loads in use at any given time in a building. The harmonic emission from several devices at the same frequency may have different phase angles, and hence the collective impact could be very different. Hence, it is essential to consider the phase angles, for the formation of models capable of providing stochastic estimates of harmonic emission in a network. However, the measurement results of harmonic aggregation may involve some uncertainties such as the impact of cable impedance and may differ from mathematical aggregation.

We conducted an experiment to assess the uncertainties and inaccuracies involved in comparing real-time measurement results and mathematical aggregation of current harmonics. For this purpose, we selected LED lamps and allowed them to warm up for at least 1 h, to eliminate any variations in their harmonic emission due to thermal stability. We measured each lamp individually and in combinations to obtain measurement results of their harmonic aggregation. The harmonic emissions of individual lamps were then mathematically aggregated and compared with the measurement results to evaluate the margins of uncertainties.

Figure 16a shows a box plot that represents the percentage difference in the aggregated magnitude of current harmonic emissions from 16 lamps between measurement data and mathematical aggregation. The difference is quite small and confirms that the mathematical aggregation replicates similar results obtained from the measurements. Note that thermal stability is an important consideration, as measurement results from thermally unstable loads may result in significant differences in aggregation. Figure 16b shows a boxplot that represents the phase angle variation between measurement aggregation and mathematical aggregation of current harmonics.

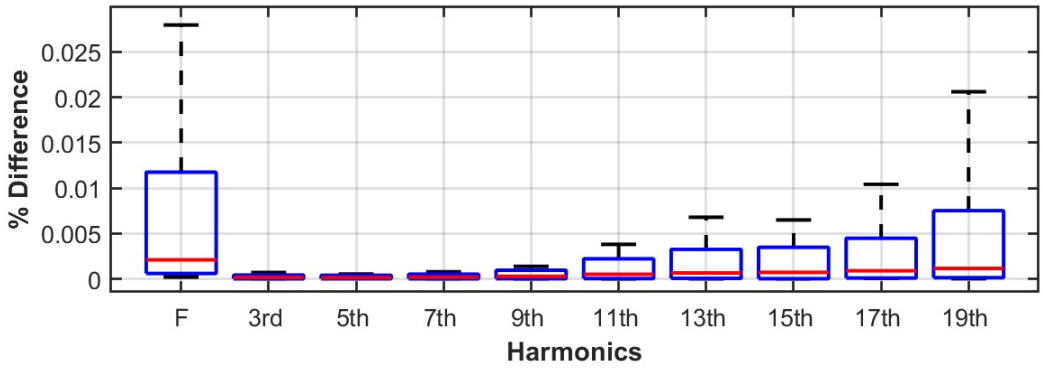

(a)

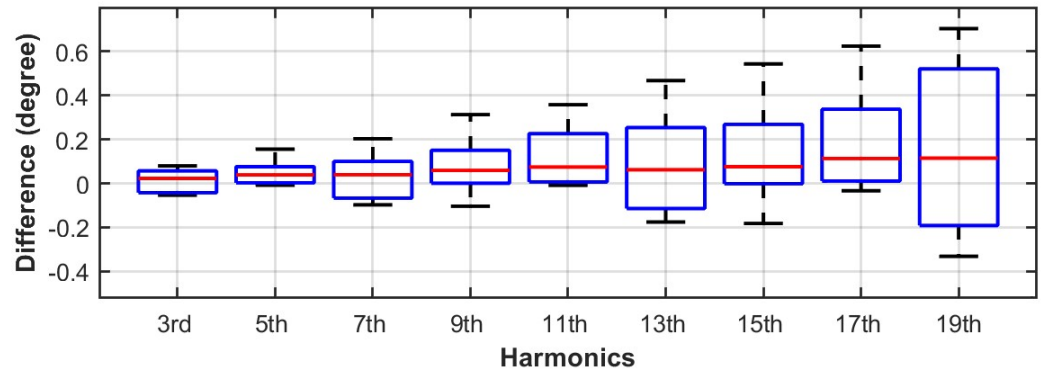

(b)

Figure 16. Difference between mathematically aggregation and measured values, (**a**) percentage magnitude difference, (**b**) absolute phase difference.

4. Conclusions

This paper provides a novel methodology for estimating and integrating various uncertainties and inaccuracies that can potentially impact the outcomes of harmonic estimation models. The study meticulously examined the effects of such uncertainties and offered a systematic approach to measure and integrate them into a harmonic estimation model.

Measurement uncertainties arise from instrument uncertainty, inaccurate measurement techniques, and variations in the measurement results. Instrument and measurement setup uncertainties were evaluated through metrological assessments. This assessment provided an accuracy margin for the measurement dataset and can be included in a harmonic estimation model.

During power quality measurements, thermal instability can lead to inaccurate readings, and up to 20% variation in THDi has been observed. The impact of thermal instability can be minimized by preheating the loads for at least 40 min before the measurements. Additionally, dynamic network conditions can affect the harmonic content of the distribution network, as variations in the voltage waveform can impact current harmonic generation. The network variations are compensated for by taking power quality measurements at various voltage waveforms. Cable impedance can also significantly affect the measurements and overall outcome of a harmonic estimation model. This could be avoided by using shorter cables during measurement. However, for the harmonic estimation model, the impact of cable impedance can be added by treating it as a stochastic variable and adding accuracy margins for both magnitude and phase variation.

The modeling methodology for the harmonic estimation model is the second category of uncertainty and inaccuracy that has a significant impact on its output estimates. The stochastic harmonic estimation model proposed in this paper is a high-resolution load

model. This high-resolution load model can replicate the real-time temporal variation in the current harmonic generation caused by the stochastic nature of the load connected to the network. It was demonstrated that empirical distributions are more effective than the conventional approach of using distribution fitted on the dataset. Modern loads employ pre-programmed usage modes to increase efficiency, but the harmonic emission spectrum during each stage varies widely, requiring full-cycle measurements for precise evaluation. Lastly, the accuracy margins of mathematical aggregation of current harmonics are evaluated and can be incorporated into the harmonic estimation model as a stochastic variable.

The proposed stochastic harmonic estimation model is capable of including the impact of uncertainty and inaccuracies arising from variations in the harmonic magnitude and phase angle of current harmonics. By accounting for these uncertainties, harmonic estimation models can produce more realistic results, providing a better understanding of the impact of harmonic emissions in future distribution networks.

Author Contributions: Conceptualization, M.N.I. and L.K.; Data curation, K.D., N.S. and M.A.; Formal analysis, M.N.I., K.D. and N.S.; Funding acquisition, N.S.; Investigation, K.D. and A.A.; Methodology, M.N.I., L.K. and A.W.A.; Project administration, N.S.; Resources, L.K. and A.W.A.; Software, M.N.I., K.D. and M.A.; Supervision, L.K. and M.A.; Validation, M.N.I., L.K. and A.A.; Visualization, A.A. and A.W.A.; Writing—original draft, M.N.I. and N.S.; Writing—review and editing, A.A., A.W.A. and M.A. All authors have read and agreed to the published version of the manuscript.

Funding: This work was supported by the Estonian Council grant (PSG142).

Institutional Review Board Statement: Not applicable.

Informed Consent Statement: Not applicable.

Data Availability Statement: Data is contained within the article.

Conflicts of Interest: The authors declare no conflict of interest.

References

1. Wang, Y.; Yong, J.; Sun, Y.; Xu, W.; Wong, D. Characteristics of Harmonic Distortions in Residential Distribution Systems. *IEEE Trans. Power Deliv.* **2017**, *32*, 1495–1504. [CrossRef]
2. Hu, H.; Shi, Q.; He, Z.; He, J.; Gao, S. Potential harmonic resonance impacts of PV inverter filters on distribution systems. *IEEE Trans. Sustain. Energy* **2015**, *6*, 151–161. [CrossRef]
3. Li, Z.; He, Z.; Song, Y.; Tang, L.; Wang, Y. Stochastic assessment of harmonic propagation and amplification in power systems under uncertainty. *IEEE Trans. Power Deliv.* **2021**, *36*, 1149–1158. [CrossRef]
4. Iqbal, M.N.; Kutt, L.; Rosin, A. Complexities associated with modeling of residential electricity consumption. In Proceedings of the 2018 IEEE 59th International Scientific Conference on Power and Electrical Engineering of Riga Technical University (RTUCON), Riga, Latvia, 12–13 November 2018; pp. 1–6. [CrossRef]
5. Roald, L.A.; Pozo, D.; Papavasiliou, A.; Molzahn, D.K.; Kazempour, J.; Conejo, A. Power systems optimization under uncertainty: A review of methods and applications. *Electr. Power Syst. Res.* **2023**, *214*, 108725. [CrossRef]
6. Singh, R.S.; Ćuk, V.; Cobben, S. Measurement-Based Distribution Grid Harmonic Impedance Models and Their Uncertainties. *Energies* **2020**, *13*, 4259. [CrossRef]
7. Xiao, X.; Li, Z.; Wang, Y.; Zhou, Y. A Practical Approach to Estimate Harmonic Distortions in Residential Distribution System. *IEEE Trans. Power Deliv.* **2021**, *36*, 1418–1427. [CrossRef]
8. Wang, Y.; Ma, H.; Xiao, X.; Wang, Y.; Zhang, Y.; Wang, H. Harmonic State Estimation for Distribution Networks Based on Multi-Measurement Data. *IEEE Trans. Power Deliv.* **2023**, *38*, 2311–2325. [CrossRef]
9. Au, M.T.; Milanović, J.V. Establishing harmonic distortion level of distribution network based on stochastic aggregate harmonic load models. *IEEE Trans. Power Deliv.* **2007**, *22*, 1086–1092. [CrossRef]
10. Zhong, Q.; Liang, J.; Xu, Z.; Meyer, J.; Wang, L.; Wang, G. Analysis of large-scale power quality monitoring data based on quantum clustering. *Electr. Power Syst. Res.* **2023**, *220*, 109366. [CrossRef]
11. Mazin, H.E.; Nino, E.E.; Xu, W.; Yong, J. A Study on the Harmonic Contributions of Residential Loads. *IEEE Trans. Power Deliv.* **2011**, *26*, 1592–1599. [CrossRef]
12. Iqbal, M.N.; Kütt, L.; Daniel, K.; Jarkovoi, M.; Asad, B.; Shabbir, N. Bivariate stochastic model of current harmonic analysis in the low voltage distribution grid. *Proc. Est. Acad. Sci.* **2021**, *70*, 190. [CrossRef]
13. Shu, Q.; He, J.; Wang, C. A Method for Estimating the Utility Harmonic Impedance Based on Semiparametric Estimation. *IEEE Trans. Instrum. Meas.* **2021**, *70*, 1–9. [CrossRef]

14. Yadav, J.; Vasudevan, K.; Meyer, J.; Kumar, D. Frequency Coupling Matrix Model of a Three-Phase Variable Frequency Drive. *IEEE Trans. Ind. Appl.* **2022**, *58*, 3652–3663. [CrossRef]
15. Jiang, C.; Salles, D.; Xu, W.; Freitas, W. Assessing the collective harmonic impact of modern residential loadspart II: Applications. *IEEE Trans. Power Deliv.* **2012**, *27*, 1947–1955. [CrossRef]
16. Ding, T.; Liang, H.; Xu, W. An Analytical Method for Probabilistic Modeling of the Steady-State Behavior of Secondary Residential System. *IEEE Trans. Smart Grid* **2017**, *8*, 2575–2584. [CrossRef]
17. Gao, S.; Li, X.; Ma, X.; Hu, H.; He, Z.; Yang, J. Measurement-Based Compartmental Modeling of Harmonic Sources in Traction Power-Supply System. *IEEE Trans. Power Deliv.* **2017**, *32*, 900–909. [CrossRef]
18. Au, M.T.; Milanović, J.V. Development of stochastic aggregate harmonic load model based on field measurements. *IEEE Trans. Power Deliv.* **2007**, *22*, 323–330. [CrossRef]
19. Salles, D.; Jiang, C.; Xu, W.; Freitas, W.; Mazin, H.E. Assessing the collective harmonic impact of modern residential loads-part I: Methodology. *IEEE Trans. Power Deliv.* **2012**, *27*, 1937–1946. [CrossRef]
20. Abdelrahman, S.; Milanović, J.V. Practical Approaches to Assessment of Harmonics Along Radial Distribution Feeders. *IEEE Trans. Power Deliv.* **2019**, *34*, 1184–1192. [CrossRef]
21. Iqbal, M.N.; Jarkovoi, M.; Kutt, L.; Shabbir, N. Impact of LED Thermal Stability to Household Lighting Harmonic Load Current Modeling. In Proceedings of the 2019 Electric Power Quality and Supply Reliability Conference (PQ) & 2019 Symposium on Electrical Engineering and Mechatronics (SEEM), Kardla, Estonia, 12–15 June 2019; pp. 1–6. [CrossRef]
22. Babaev, S.; Cobben, S.; Cuk, V.; Brom, H.V.D. Online Estimation of Cable Harmonic Impedance in Low-Voltage Distribution Systems. *IEEE Trans. Instrum. Meas.* **2020**, *69*, 2779–2789. [CrossRef]
23. Geng, X.; Su, G.; Lu, W.; Xiong, Z.; Gao, Y.; Bu, X.; Yan, H.; Du, S. Study on the Harmonic Amplification Influence of DC Inverter Substation With Cable Outgoing Line on the Receiving-end Power Grid. In Proceedings of the 2021 3rd Asia Energy and Electrical Engineering Symposium (AEEES), Chengdu, China, 26–29 March 2021; pp. 448–453. [CrossRef]
24. Herman, R.; Kritzinger, J. The statistical description of grouped domestic electrical load currents. *Electr. Power Syst. Res.* **1993**, *27*, 43–48. [CrossRef]
25. Daniel, K.; Kutt, L.; Iqbal, M.N.; Shabbir, N.; Parker, M.; Jarkovoi, M. Waveform Variation Defined Model for Harmonic Current Emissions Including Cross-Order Supply Voltage Harmonics Influence. *IEEE Access* **2023**, *11*, 42276–42289. [CrossRef]
26. Singh, R.; Pal, B.C.; Jabr, R.A. Statistical representation of distribution system loads using Gaussian mixture model. *IEEE Trans. Power Syst.* **2010**, *25*, 29–37. [CrossRef]